Inflammation Research (2026) 75:29
https://doi.org/10.1007/s00011-026-02184-y

Inflammation Research

RESEARCH

Palmitic acid aggravates atopic dermatitis by regulating SGK1/NEDD4L-involved cutaneous neuroimmune inflammation through driving TRPV1 and MRGPRB2 S-palmitoylation

Bangtao Chen[1] · Jing Yang[1,2] · Tingting Song[2] · Weiyu Wu[1] · Fei Hao[2] · Zhi Yang[2]

Received: 20 October 2025 / Revised: 28 December 2025 / Accepted: 5 January 2026

Abstract

Objective To determine how cutaneous palmitic acid (PA) modulates transient receptor potential vanilloid-1(TRPV1) in nociceptor and dorsal-root-ganglions (DRGs), and Mas-related G protein-coupled receptor B2 (MRGPRB2) in mast cells (MCs), and to investigate their associations with serum- and glucocorticoid-regulated kinase-1 (SGK1)/neural precursor cell expressed developmentally down regulated 4-like (NEDD4L) in atopic dermatitis (AD).

Methods AD was induced in mice with *nedd4l* or *sgk1* conditional knock-out(cKO) in nociceptor, *mrgprb2*, *nedd4l*, or *sgk1* cKO in MCs. Intradermal PA, substance P(SP), or pan-palmitoylation inhibitor 2BP was administered. Isolated DRGs and mouse bone-marrow-derived-MCs (mBMMCs) were used.

Results Cutaneous PA levels were increased in AD mice.PA intradermal injection promoted a $TRPV1^+$ nociceptor-SP-MCs MRGPRB2-tryptase-AD axis. *nedd4l* cKO in nociceptor up-regulated cutaneous SP expression, which was further enhanced by PA. *sgk1* cKO in nociceptor slightly reduced SP levels, which were further decreased by PA or 2BP. SP levels in mice with *nedd4l* or *sgk1* cKO in MCs were increased by PA. In DRGs, supernatants from MC903-treated keratinocytes induced SGK1 and NEDD4L phosphorylation, TRPV1 S-palmitoylation, and SP production, all of which were up-regulated by PA; total and S-palmitoylated TRPV1 levels and SP production were increased following *nedd4l* knockdown, whereas they were slightly reduced following *sgk1* knockdown and further decreased by PA. SP induced weak phosphorylation of SGK1 and NEDD4L in MCs. SP induced MRGPRB2 S-palmitoylation and tryptase release in *wild-type*, *nedd4l* or *sgk1* knock-out MCs, and these effects were enhanced by PA; 2BP caused MRGPRB2 reduction in *wild-type* and *sgk1* knock-out MCs.

Conclusions The increased cutaneous PA exacerbates AD by promoting TRPV1 S-palmitoylation and SP production in nociceptor, followed by MRGPRB2 S-palmitoylation and tryptase release in MCs. S-palmitoylation promotes TRPV1 whereas inhibits MRGPRB2 reduction via lysosome when NEDD4L and its upstream SGK1 are not phosphorylated.

Keywords S-palmitoylation · Palmitic acid · Atopic dermatitis · TRPV1 · MRGPRB2 · NEDD4L

Introduction

Atopic dermatitis (AD) is a well-recognised Th2-inflammation-driven pruritic dermatosis with a global prevalence of approximately 3.96% in children and 1.95% in adults [1]. It is well established that the cutaneous neuroimmune circuit represents a central pathophysiological mechanism underlying recalcitrant chronic itching in AD [2, 3]. Internal and external factors influencing the itch circuit [i.e. peripheral sensory nerves-dorsal root ganglions (DRGs)-spinal cord-brain], together with skin-resident cells, synergistically determine AD degree. These factors especially underlie AD heterogeneity by differentially activating diverse membrane

Bangtao Chen and Jing Yang have contributed equally to this work.

Responsible Editor: John Di Battista.

✉ Zhi Yang
650814@hospital.cqmu.edu.cn

[1] Department of Dermatology, School of Medicine, Chongqing University Three Gorges Hospital, Chongqing University, Chongqing 404100, People's Republic of China

[2] Department of Dermatology, Third Affiliated Hospital of Chongqing Medical University, Chongqing 401120, People's Republic of China

Published online: 02 February 2026

receptors and ion channels on sensory nerve endings, keratinocytes, and mast cells (MCs). Among these, transient receptor potential (TRP) superfamily and the recently identified Mas-related G protein-coupled receptor (MRGPR) further enhance understanding of cutaneous neuroinflammation in AD [4].

Serum- and glucocorticoid-regulated kinase 1 (SGK1)/neural precursor cell- expressed, developmentally downregulated 4-like (NEDD4L) signaling is widely involved in physiological homeostasis and diseases progression through multiple mechanisms. One such mechanism is that NEDD4L targets multiple proteins for ubiquitination and then the ubiquitinated proteins are degraded via proteasomal or lysosomal pathways, as observed during IgE-mediated activation of mouse bone marrow-derived mast cells (mBMMCs) [5]; however, the ubiquitination activity of NEDD4L is negatively regulated by SGK1 through phosphorylating NEDD4L [6].Studies investigating the role of cutaneous SGK1 in AD, using animal models and clinical skin lesions, have yielded inconsistent results, likely due to variations in expression modulation across different skin cell types [7–9]. In addition, no in vivo studies have investigated the role of NEDD4L signaling in AD; however, evidence indicates that cutaneous NEDD4L signaling negatively regulates keloid fibroblasts proliferation and migration, keratinocyte hyperplasia and skin tumorigenesis [10–12]. Chen et al. previously demonstrated the role of SGK1/NEDD4L signalling in IgE- and bacterial DNA-mediated MCs activation in vitro; however, in vivo validation in the context of AD is lacking [13]. SGK1 and NEDD4L are widely expressed in spinal cord and brain. Liu et al. showed that nerve growth factor contributes to chronic post-surgical pain by increasing the voltage-gated sodium channel Nav1.7 in DRGs through SGK1 dependent NEDD4L phosphorylation [14], thereby confirming the expression of SGK1 and NEDD4L in nociceptors. However, the effects of SGK1/NEDD4L signaling in sensory nerve or MCs on AD development and specific mechanism (especially the identification of target proteins) remain unexplored.

Available evidence demonstrates that TRPV1, which is widely expressed in various skin cells, including keratinocytes, T cells and sensory nerves, is an important molecule in pruritus signaling and/or skin inflammation in AD and other itch related dermatoses [15, 16]. $TRPV1^+$ sensory nerves or nociceptors mediating non-histaminergic itching and allergic skin inflammation mainly through the production of SP in various inflammatory skin disease models are well characterised [15, 17, 18]. Resiniferatoxin(RTX)-mediated ablation of $TRPV1^+$ nociceptor shows excellent anti-itch and anti-inflammatory effects [19, 20]. Recently, Zhang et al. found that intra-plantar carrageenan injection could initiate the S-palmitoylation of the TRPV1 protein in mouse DRGs in vivo and confirmed that the palmitoyl acyltransferase zinc finger DHHC domain-containing (zDHHC)-4 catalysed S-palmitoylation at four cysteine residues (C157, C362, C390, and C715) of TRPV1 in HEK293T cells in vitro, thereby facilitating inflammatory pain relief by driving TRPV1 degradation in lysosomes rather than proteasomes [21]. The finding that S-palmitoylation drives TRPV1 instability may provide important mechanistic insights into $TRPV1^+$ nociceptor in skin neuroimmune inflammation in AD. TRPV1 in non-neuronal cells has been found to interact with SGK1, and its stability is downregulated upon SGK1 knockdown [22], leading to the speculation that SGK1 loss may promote NEDD4L-mediated lysosomal degradation of TRPV1.

SP is a neuropeptide that orchestrates skin neurogenic inflammation via MCs-expressing neurokinin-1 receptor and MRGPRX2, with recent evidence indicating a more prominent role for MRGPRX2 [19, 23, 24]. MRGPRB2 is the mouse orthologs of human MRGPRX2. In contrast to IgE-mediated activation, SP-mediated MRGPRX/B2 activation predominantly induces the release of tryptase rather than histamine, with tryptase subsequently initiating skin Th2-inflammation in AD [25]. Wang et al. discovered that β-arrestin-2 and β-arrestin-1 mediate MRGPRX2 signal termination by inhibiting extracellular signal-regulated kinase phosphorylation and promoting MRGPRX2 internalisation, respectively [26]. Several studies have shown that β-arrestin-1 or -2 can recruit NEDD4/NEDD4L to facilitate the NEDD4/NEDD4L-mediated ubiquitination and degradation of target G protein-coupled receptor other than MRGPRX2 [27–29]. In our preliminary experiments, molecular docking analysis indicated a high likelihood of interaction between NEDD4L and MRGPRX/B2, and GPS-Palm software predicted two putative S-palmitoylation sites (C168 and C211) in the MRGPRX2 protein and two sites (C175 and C338) in MRGPRB2 [30]. Therefore, analogous to its role in TRPV1 stability, NEDD4L may also regulate MRGPRX/B2 abundance, potentially influenced by S-palmitoylation.

Evidence on the role of S-palmitoylation in AD is limited; only Chen et al. demonstrated that ZDHHC13-mediated protein S-palmitoylation in the skin maintains the integrity of multiple barriers functions and protects mice from microbe-driven AD [31]. Protein S-palmitoylation is an emerging and important post-translational modification in which palmitic acid (PA), a 16-carbon long-chain (C16:0) saturated fatty acid, is covalently attached to cysteine residues in proteins through a thioester bond. PA is one of the major medium- and long- chain fatty acids (ML-CFAs) in tissues, and several studies have examined the alterations in ML-CFAs (including PA) in clinical lesions from patients with AD; however, the conclusions have been inconsistent

[32]. In addition, research evidence regarding PA alteration in animal AD models and their potential mechanisms or roles is currently unavailable. Therefore, this study aimed to determine alteration in cutaneous PA and its role in AD-like mice, with a focus on TRPV1 and MRGPRB2 S-palmitoylation, and to further explore its relationship with SGK1/NEDD4L signaling in sensory nerves and MCs.

Materials and methods

Mice

All animal experiments and procedures were approved by the Ethics Committee of Chongqing University Three Gorges Hospital. All experiments were conducted in accordance with the national guidelines on animal protection, *Laboratory animal - Guideline for ethical review of animal welfare* (GB/T 35892−2018, China). Chinese Cyagen Biosciences Inc (Suzhou, Jiangsu Province) provided the wild-type (*wt*)-, *nedd4l* flox(f/f)-, *sgk1* flox(f/f)-, *mrgprb2* flox(f/f)-, Cmv^{Cre} mice and $Advillin^{Cre}$- C57BL/6J mice. $Capa3^{Cre}$ C57BL/6J mice were kindly provided by professor Songmei Geng (Xi'an Jiaotong University).Mice with conditional knockout (cKO) of *nedd4l* or *sgk1* in sensory nerve were generated by mating *nedd4l*(f/f) and *sgk1*(f/-) mice with $Advillin^{Cre}$ mice, respectively. cKO *nedd4l*, *sgk1*, or *mrgprb2* in MCs was achieved by mating *nedd4l*(f/f), *sgk1*(f/f), or *mrgprb2* (f/f) mice with $Capa3^{Cre}$ mice, respectively. Mating *sgk1*(f/f)/*nedd4l*(f/f) mice with $Capa3^{Cre}$ mice produced offspring mice with double knockout(KO) of *sgk1* and *nedd4l* in MCs. Mating *mrgprb2*(f/f)/*nedd4l*(f/f) mice or *mrgprb2*(f/f)/*sgk1*(f/f) mice with Cmv^{Cre} mice produced offspring mice with double KO of *mrgprb2* and *nedd4l* or *mrgprb2* and *sgk1*, respectively.

All mice were bred and housed in ventilated cages on the same housing unit (room temperature:25 ± 2 ◦C, humidity:50 ± 5%, light/dark:12 h/12 h) in specified pathogen free room.

Reagents

MC903(#HY-10001, MCE), SP(# HY-P0201, MCE), PA(#HY-N0830, MCE), 2-Bromopalmitate (2BP; #21604, Sigma-Aldrich), capsazepine (#HY-15640,MCE), RTX (#T34295, TargetMol), Benzamidine hydrochloride(Ben; #HY-W018781, MCE), Bafilomycin A1 (BafA1; # S1413, Selleck), IP-Acyl-biotin exchange (ABE) Palmitoylation Kit (#AM10314, AIMS), enhanced chemiluminescence detection kit (#WBKLS, Millipore), hematoxylin and eosin (HE) kit (#DH0020, Leagene). Enzyme-linked immunosorbent assay (ELISA) kits included mouse IL-1β(#E-EL-M0037, Elabscience), mouse IL-6(#E-EL-M0044, Elabscience), mouse IL-13 (#MM-0173M2, MEIMIAN), mouse thymic stromal lymphopoietin (TSLP; #MM-45118M2, MEIMIAN), mouse TNF-α (#MM-0132M2, MEIMIAN), mouse SP(#E-EL-0067, Elabscience), mouse gastrin-releasing peptide (GRP, #EKC36933,Biomatik), mouse tryptase(#EKU07923, Biomatik), and mouse total IgE (#ab157718, Abcam). Antibodies included anti-NEDD4L (#A8085, ABclonal), anti-phosphorylated NEDD4L (Ser448, #AP0843, ABclonal), anti-GAPDH (#A19056, Abclonal), anti-β-Tubulin (#A12289, Abclonal), anti-SGK1 (#12103, CST), anti-phosphorylated SGK1 (Ser78, #5599, CST), anti-TRPV1(#AF8250, Beyotime), anti-Flag(#MA5-50638, Invitrogen).

Ablation of $TRPV1^+$ nociceptors in mice

To ablate $TRPV1^+$ nociceptors, 4-week-old C57BL/6J mice were subcutaneously injected with RTX (30 μg/kg, 70 μg/kg and 100 μg/kg) in 100 μL PBS for 3 consecutive days. Control mice were injected with an equal volumes of solvent(SVT). Four weeks later, the mice were used for subsequent experiments.

AD mouse model and interventions

MC903 (45 μM; 20 μL/cm^2) was topically applied to the exposed nape or ear of the mice for 10–14 consecutive days to induce AD-like dermatitis. Each group contained 4 male and 4 female mice. During MC903 application, PA, 2BP, SP, or Ben dissolved in 30 μL saline (PA or 2BP dissolved in 15 μL saline in ear-AD model), were administered intradermally, whereas capsazepine, dissolved in 100 μL saline, was administered subcutaneously on the indicated days. Control mice received an intradermal injection of an equal volume of SVT. Additionally, the effect of intradermal injection of 2BP at different doses on epidermal thickness in AD-like lesions from nape-AD model was predetermined (Supplementary Fig. 1). Furthermore, 3% pentobarbital sodium (5 μL/g) was administered intraperitoneally to induce anesthesia, after which the relevant samples were collected.

Plasmid construction

To construct mouse MRGPRB2 expression plasmid, a full-length mouse MRGPRB2 cDNA was synthesised by GenScript Biotech Co.,Ltd (Nanjing, China), and the cDNA was then inserted into a modified pcDNA3.1 vector containing a C-terminal Flag tag using homologous recombination.

mBMMCs, DRGs or keratinocytes isolation and culture

Mouse bone marrow-derived mast cells (mBMMCs) precursors were isolated from the tibias and femurs of 10–12-week-old *mrgprb2* (f/f)·Cmv^{Cre}, *mrgprb2* (f/f)/*nedd4l*(f/f)·Cmv^{Cre} mice or *mrgprb2*(f/f)/*sgk1*(f/f)·Cmv^{Cre} mice by flushing with sterile Hanks' Balanced Salt Solution, as previously described by Meurer et al. [33]. Then, the cells were cultured in RPMI 1640 medium supplemented with 10% FBS, 1% Pen-Strep, 0.05 mM β-mercaptoethanol, 25 mM HEPES, 1 mM sodium pyruvate, 0.1 mM non-essential amino acids, 2 mM L-glutamine and 30 ng/mL recombinant mouse IL-3. After culturing at 37 °C in 5% CO_2 for 4–6 weeks, flow cytometry was applied to confirm the purity of mBMMCs using Brilliant Violet 421™ anti-mouse CD117 and PE anti-mouse FcεRIα prior to transfection and subsequent treatments.

DRGs were isolated and cultured as described by Shekarabi et al. [34], with minor modifications. Briefly, adult *wt* or gene-edited C57BL/6J mice were euthanatized with isoflurane and then decapitated. DRGs connected to the spinal cord were dissected, the attached nerves and connecting spinal cord tissues were then removed using sterile ophthalmic scissors and tweezers under a microscope. After rinsing with ice-cold Ham's F12 medium, the DRGs were digested with collagenase type II (240 U/mL) and trypsin (10000 U/mL) in Ham's F12 for 60 min and 10 min at 37 °C, respectively. DRGs suspended in Ham's F12 were gently dispersed by mechanical trituration with a sterile pipette tip and collected by centrifugation (500 × g for 5 min), after which they were then seeded onto poly-L-Lysine-coated culture plates containing Ham's F12 medium supplemented with 10% heat-inactivated FBS, 1 mM L-glutamine, 1% Pen-Strep, and 50 ng/mL nerve growth factor.

Mouse keratinocytes were isolated from the tail skin of 10–12-week-old *wt* mice, as described by Li et al. [35]. The cells were cultured in Mouse Epidermal Keratinocyte Cell Complete Medium(CM-M094, Procell).

In addition, in vitro experiments involved the application of MC903, SP, PA, 2BP and BafA1 as indicated in the figures.

Protein palmitoylation assay

S-palmitoylation levels of TRPV1 protein in cultured DRGs and MRGPRB2·Flag protein in mBMMCs were analysed using the ABE according to the instructions for IP-ABE Palmitoylation Kit. Briefly, the harvested cells were lysed in lysis buffer and then incubated with protein A/G beads and anti-TRPV1 or anti-Flag overnight at 4 °C. N-ethylmaleimide (NEM) was added to the solution to block the unmodified cysteines for 30 min at room temperature (RT). Then, the beads were washed, after which half of them were incubated with hydroxylamine (HA+) and the remaining half with standard lysis buffer (HA-) for 1 h at RT. After washing, the beads were treated with thiol-reactive biotin reagent for 1 h at RT. The immunoprecipitated samples were analysed by western blotting using streptavidin-HRP antibody.

Immunoprecipitation and western blotting

For co-immunoprecipitation, the harvested DRGs or mBMMCs from in vitro experiments were lysed in ice-cold RIPA buffer containing protease and phosphatase inhibitors for 20 min on ice and then centrifugated at 12,000 × g for 15 min at 4 °C. The supernatants were incubated with Pierce Protein G Agarose and the appropriate primary antibody or IgG control on the rotating frame overnight at 4 °C. The beads were then washed five times with RIPA buffer on ice and finally boiled in sample buffer for western blotting. The collected supernatants without immunoprecipitation were also boiled in loading buffer for SDS–PAGE. The details for western blotting and protein visualization were described previously [13]. Primary antibodies used included anti-SGK1, anti-NEDD4L, anti-TRPV1, and anti-Flag.

Gas chromatography mass spectrometry (GC-MS)

A total of 36 ML-CFAs in skin lesion and spinal cord were simultaneously determined by GC-MS, as described previously [36].

ELISA

Serum IgE and tissue levels of IL-1β, IL-6, TNF-α, SP, tryptase, IL-13, and TLSP were determined by ELISA using the corresponding commercial kits following the manufacturer's instructions.

Histological stain

Fresh skin lesions were cut into 0.5 × 0.5 cm^2 sections, fixed in 4% paraformaldehyde for 24 h, and embedded in paraffin. Deparaffinised and rehydrated slices were stained with HE to measure epidermal thickness and assess the inflammatory infiltration. Immunofluorescence was performed to assess the expression and co-localisation of dermal TRPV1, SGK1 and NEDD4L.

Statistical analyses

Bioinformatic analyses of the GC–MS data were performed using a free online platform of Majorbio cloud platform (cloud.majorbio.com). GraphPad Prism 5.0® software package (San Diego, California) was used for statistical analyses. One-way ANOVA followed by Bonferroni's multiple-comparison post hoc tests were used to analyse differences between groups. Student's t-test was used for determining differences between two groups. Two-sided $P<0.05$ was considered statistically significant.

Results

Cutaneous and spinal inflammation or ML-CFAs in AD-like mice

As shown in Table 1, in the nape-AD model, compared with the SVT group, serum IgE and skin levels of SP, tryptase, TSLP, and IL-13 were significantly increased in varying degrees, significant increases in spinal GRP, IL-1β, IL-6 and TNF-α levels were also observed, spinal SP was only slightly up-regulated in the MC903-treated group. In ear-AD model, compared to SVT group, serum IgE, spinal GRP, skin SP, tryptase, TSLP, and IL-13 contents were also increased in varying degrees, while spinal SP, IL-1β, IL-6 and TNF-α levels were not altered in MC903-treated group. More specifically, elevations in skin inflammatory mediators in the MC903-treated ear were remarkably higher than those in the MC903-treated nape, whereas the elevation in spinal GRP was significantly lower.

A total of 36 ML-CFAs in the skin and spinal cord were determined by GC-MS. In the nape-AD model, spinal C16:0, C18:0, C18:1n9t, C20:1, and C22:6n3 (published data), as well as skin C16:0, C16:1, and C18:1n9c, were significantly increased in MC903-treated mice compared with those in the SVT-treated mice (Fig. 1A). In the ear-AD model, skin C16:0, C18:0, C18:1n9t, C20:1, C20:4n6, and C22:6n3 were also significantly increased in MC903-treated mice compared with those in the SVT-treated mice (Fig. 1B), while all determined ML-CFAs in the spinal cord were unchanged (Fig. 1C). Moreover, the concentrations of major ML-CFAs, including C16:0, in the skin were significantly higher in the MC903-treated nape than in the ear.

Palmitoylation intervention in the AD phenotype

To determine the role of skin palmitoylation in the AD phenotype, PA (C16:0), the pan-palmitoylation inhibitor 2BP, or the corresponding SVT, were intradermally injected on days 3, 6, 9 during MC903 challenge. As shown in Table 2, epidermal thickness, skin levels of SP, tryptase, TSLP, IL-13, and spinal GRP level were significantly increased in mice receiving PA, whereas these parameters were significantly decreased following 2BP administration in both ear- and nape-AD models. Moreover, in the nape-AD model, PA administration also caused marked increases in spinal SP, IL-1β, IL-6 and TNF-α levels, whereas 2BP administration resulted in significant decreases in spinal SP and TNF-α level. Spinal SP, IL-1β, IL-6 and TNF-α levels were not altered in mice receiving PA or 2BP administration compared with that using the SVT in the ear-AD model. Serum IgE levels remained similar in mice receiving PA or 2BP challenge in both models.

TRPV1$^+$ nociceptors ablation suppresses the skin SP-tryptase-TSLP axis in AD

In nape-AD mice, ablation of TRPV1$^+$ nociceptors by RTX significantly reduced epidermal thickness and skin levels of SP, tryptase, and TSLP; as expected, these changes were

Table 1 Cutaneous and spinal inflammation in MC903-induced AD models

Groups indicators	Nape		Ear	
	SVT	MC903	SVT	MC903
Epid thickness	20.22 ± 3.06	73.27 ± 2.70***	21.20 ± 4.74	61.72 ± 5.82***
Serum IgE	99.01 ± 24.15	239.78 ± 33.89***	84.59 ± 21.06	266.66 ± 47.35***
Skin SP	9.18 ± 2.65	18.29 ± 6.89**	12.77 ± 3.79	25.33 ± 5.28***
Skin tryptase	20.01 ± 5.79	49.28 ± 17.32***	41.84 ± 10.17	99.40 ± 18.76***
Skin TSLP	70.27 ± 18.83	149.71 ± 28.79***	107.11 ± 19.49	201.53 ± 29.10***
Skin IL-13	1.06 ± 0.18	1.73 ± 0.22***	1.11 ± 0.23	2.14 ± 0.43***
Spinal SP	90.16 ± 15.38	109.84 ± 12.47	78.67 ± 17.55	83.35 ± 21.84
Spinal GRP	72.97 ± 13.40	137.85 ± 23.71***	66.91 ± 15.28	106.12 ± 22.37***
Spinal IL-1β	54.89 ± 14.14	89.18 ± 13.18***	59.93 ± 14.23	61.02 ± 18.02
Spinal IL-6	15.69 ± 6.34	27.29 ± 10.82**	18.93 ± 6.36	19.31 ± 5.76
Spinal TNF-α	50.22 ± 10.17	82.49 ± 25.27**	52.34 ± 15.66	60.83 ± 28.41

MC903 or SVT was topically applied to the exposed nape or ear areas of 8–10-week-old mice for 14 consecutive days, the mice were then anesthetized and related samples were obtained. All indicators are measured in pg/mg, except for epidermal(Epid) thickness(μm) and serum IgE(ng/mL). Statistics: One-way ANOVA + Bonferroni's tests, ** $P<0.01$, *** $P<0.001$

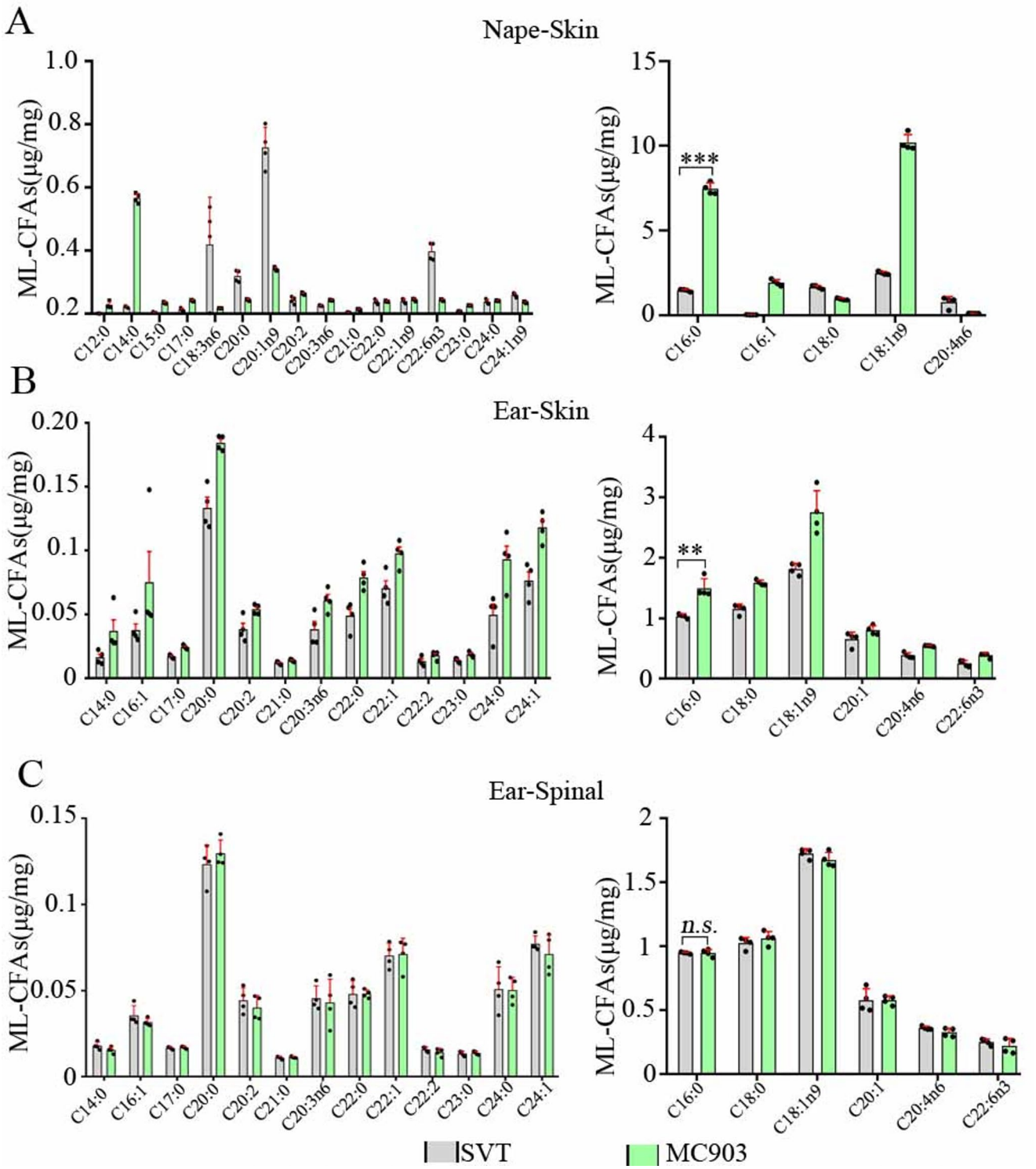

Fig. 1 Comparisons of skin and spinal ML-CFAs levels in the murine AD models. The levels of skin ML-CFAs in the nape-AD model **A**, skin ML-CFAs **B** and spinal ML-CFAs **C** in the ear-AD model are shown. Statistics: Student-t tests, $^{**}P < 0.01$, $^{***}P < 0.001$, n.s. $P > 0.05$

reversed by intradermal injection of exogenous SP (Fig. 2A–E). Meanwhile, in nape-AD mice with TRPV1^{+} nociceptors ablation, intradermal injection of SP combined with Ben (tryptase antagonist) or with 2BP were administered. Compared with SP-treated group, Ben markedly suppressed skin TSLP levels and epidermal thickness without affecting skin tryptase levels, whereas 2BP suppressed skin tryptase and TSLP levels as well as epidermal thickness (Fig. 2A–E).

Table 2 Effect of intradermal injection of PA or 2BP on AD-like dermatitis

Groups indicators	Nape			Ear		
	MC903 + SVT	MC903 + PA	MC903 + 2BP	MC903 + SVT	MC903 + PA	MC903 + 2BP
Epid thickness	72.88 ± 3.45	92.38 ± 4.00***	42.32 ± 4.36***	62.07 ± 5.50	100.98 ± 10.08***	32.41 ± 4.47***
Serum IgE	246.45 ± 48.72	244.06 ± 40.77	223.94 ± 43.85	267.51 ± 52.80	276.66 ± 58.01	254.93 ± 44.01
Skin SP	22.56 ± 5.14	32.92 ± 7.79**	14.07 ± 3.19*	28.35 ± 5.59	37.28 ± 4.13**	19.86 ± 5.44**
Skin tryptase	56.45 ± 17.06	81.72 ± 20.55*	28.82 ± 10.34**	92.88 ± 13.79	188.42 ± 35.51***	65.13 ± 13.56*
Skin TSLP	188.93 ± 39.06	248.83 ± 40.88**	138.57 ± 22.90*	215.42 ± 29.63	268.33 ± 36.58**	126.34 ± 12.76***
Skin IL-13	1.76 ± 0.27	2.71 ± 0.34***	1.30 ± 0.32*	2.42 ± 0.33	2.99 ± 0.32*	1.75 ± 0.53**
Spinal SP	108.93 ± 13.31	129.62 ± 12.37**	91.32 ± 12.41*	74.65 ± 28.62	83.86 ± 18.55	75.49 ± 20.22
Spinal GRP	138.16 ± 26.50	179.19 ± 45.72*	87.87 ± 24.17*	111.42 ± 12.24	133.26 ± 25.00*	89.34 ± 8.76*
Spinal IL-1β	87.24 ± 10.46	109.18 ± 20.83**	80.76 ± 15.29	63.99 ± 14.94	59.16 ± 13.61	65.28 ± 19.63
Spinal IL-6	25.64 ± 7.90	38.72 ± 8.90*	19.59 ± 6.54	19.70 ± 6.92	21.06 ± 5.85	20.16 ± 7.51
Spinal TNF-α	84.08 ± 16.90	114.88 ± 17.07**	59.31 ± 14.29*	62.87 ± 18.37	64.70 ± 23.39	60.29 ± 17.55

MC903 was topically applied to the exposed nape or ear areas of 8–10-week-old mice for 12 consecutive days. On days 3, 6, 9, the mice received intradermal injection of PA (2 μg/cm^2), 2BP (2 μg/cm^2) or equivalent volume of SVT. All indicators are measured in pg/mg, except for epidermal(Epid) thickness(μm) and serum IgE(ng/mL). Statistics: One-way ANOVA + Bonferroni's tests, *$P < 0.05$, **$P < 0.01$, ***$P < 0.001$

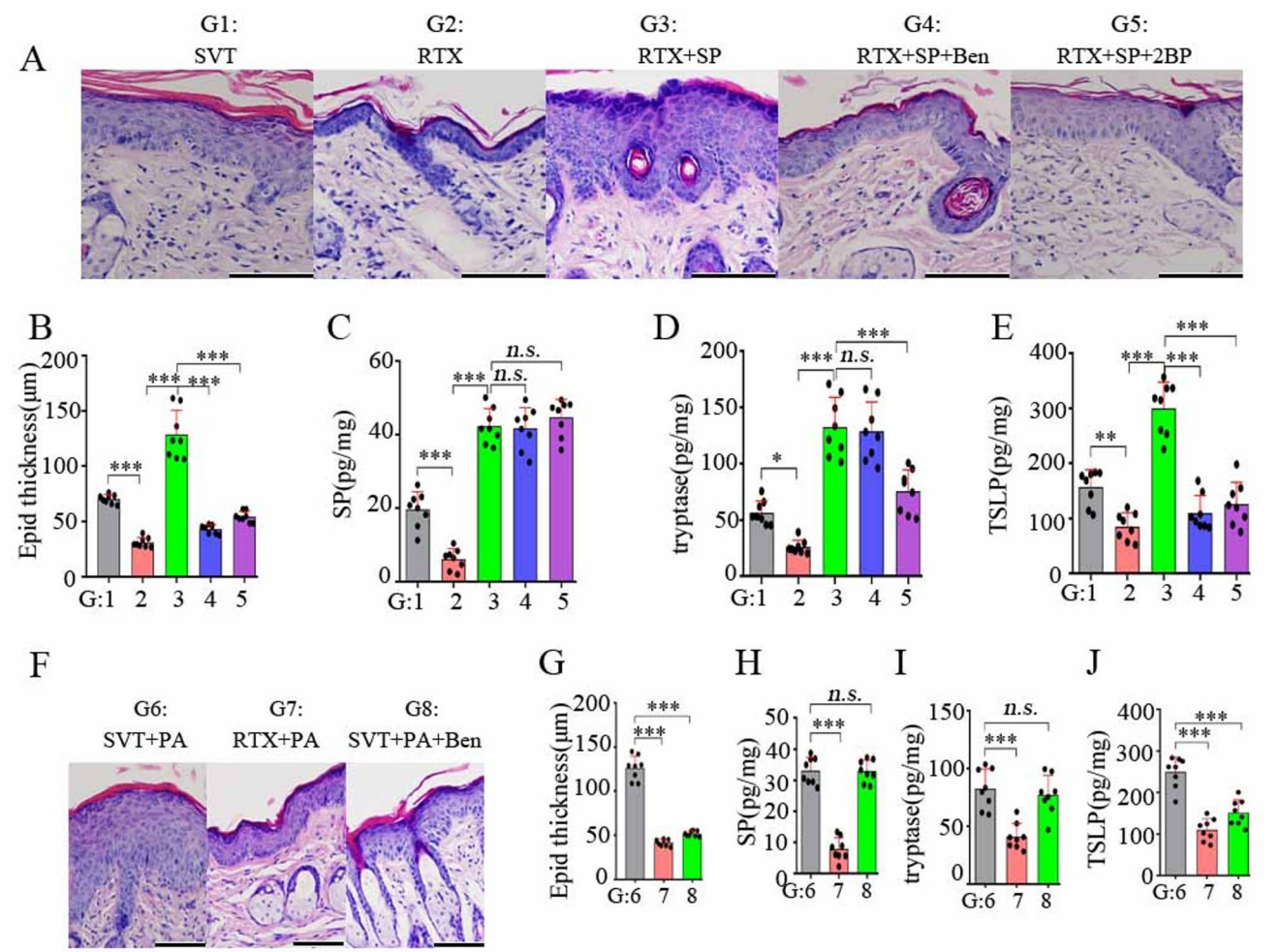

Fig. 2 Role of TRPV1$^+$ nociceptors in MC903/PA-induced dermatitis. RTX (30,70,100 μg/kg) was injected subcutaneously into mice with 4-week-old for 3 consecutive days. Four weeks later, the mice were topically treated with MC903 for 12 days, and SP (10 ng/cm^2), SP + 2BP (2 μg/cm^2), or SP + Ben (2 μg/cm^2) were intradermally injected on days 3, 6, 9. **A** HE staining of the skin lesions (scale bar = 100 μm), **B** epidermal(Epid) thickness, **C** skin SP, **D** skin tryptase, **E** skin TSLP are shown. In addition, SVT- or RTX-treated mice were topically treated with MC903 for 12 days, and PA (2 μg/cm^2) or PA + Ben (2 μg/cm^2) were intradermally injected on days 3, 6, 9. **F** HE staining of the skin lesions (scale bar = 100 μm), **G** epidermal(Epid) thickness, **H** skin SP, **I** skin tryptase, **J** skin TSLP are shown. Statistics: One-way ANOVA + Bonferroni's tests, *$P < 0.05$, **$P < 0.01$, ***$P < 0.001$, n.s. $P > 0.05$

In nape-AD mice with PA administration intradermally (Fig. 2F), RTX-mediated TRPV1$^+$ nociceptors ablation also reduced epidermal thickness and skin levels of SP, tryptase and TSLP; additionally, Ben supplementation reduced skin TSLP levels and epidermal thickness without affecting skin SP and tryptase release. In addition, subcutaneous injection of capsazepine, a TRPV1 antagonist, also partially reduced MC903-induced epidermal thickening and skin SP up-regulation in *wt* mice (Supplementary Fig. 2). These data confirm that PA-mediated AD exacerbation relies on TRPV1$^+$ nociceptors, which are critical for skin SP upregulation.

Communication between TRPV1$^+$ nerves and MCs via MRGPRB2

To further investigate whether MRGPRB2 in MCs plays a role in PA-mediated AD exacerbation and whether deletion of *mrgprb2* in MCs further promotes 2BP-mediated AD relief, mice with cKO of *mrgprb2* in MCs were used. Under MC903 + PA treatment, skin SP levels were unchanged, whereas skin tryptase and TSLP and epidermal thickness were alleviated in *mrgprb2*(f/f)·Capa3^{Cre} mice compared with that in the *mrgprb2*(f/f) mice. In contrast, under MC903 + 2BP treatment, skin SP levels remained similar, whereas skin tryptase, TSLP and epidermal thickness were only slightly alleviated in *mrgprb2*(f/f)·Capa3^{Cre} mice compared with that in the *mrgprb2*(f/f) mice (Fig. 3). These data suggest that MCs-specific MRGPRB2 signalling does not affect SP release from TRPV1$^+$ nociceptors but serves as a key mediator in promoting skin neuro-inflammation and AD phenotype under PA treatment, while appearing to have no significant role under 2BP treatment.

SGK1/NEDD4L pathway regulating TRPV1 S-palmitoylation and SP expression in DRGs in vitro

Advillin is selectively expressed in peripheral sensory neurons and DRGs [37], and it has been applied to generate Cre-mice for gene editing in sensory neurons. Immunofluorescence analysis showed that Advillin-positive neurons in the dermis of MC903-treated nape also expressed TRPV1(Fig. 4); furthermore, dermal TRPV1, NEDD4L, and SGK1 exhibited co-localisation (Fig. 5A). DRGs isolated from *nedd4l*(f/f) or *nedd4l*(f/f)·Advillin^{Cre} mice were cultured and stimulated with supernatants collected from MC903-treated keratinocytes(SCMK). CO-IP analysis of protein lysates from these DRGs, using anti-NEDD4L or anti-SGK1 for immunoprecipitation, demonstrated interactions among TRPV1, NEDD4L, and SGK1 interacted; notably, the interaction between SGK1 and TRPV1 was not affected by *nedd4l* knockdown (Fig. 5B).

Next, levels of SGK1 and NEDD4L phosphorylation, TRPV1 S-palmitoylation, and supernatant SP were determined in *wt* DRGs treated with MC903 in combination with

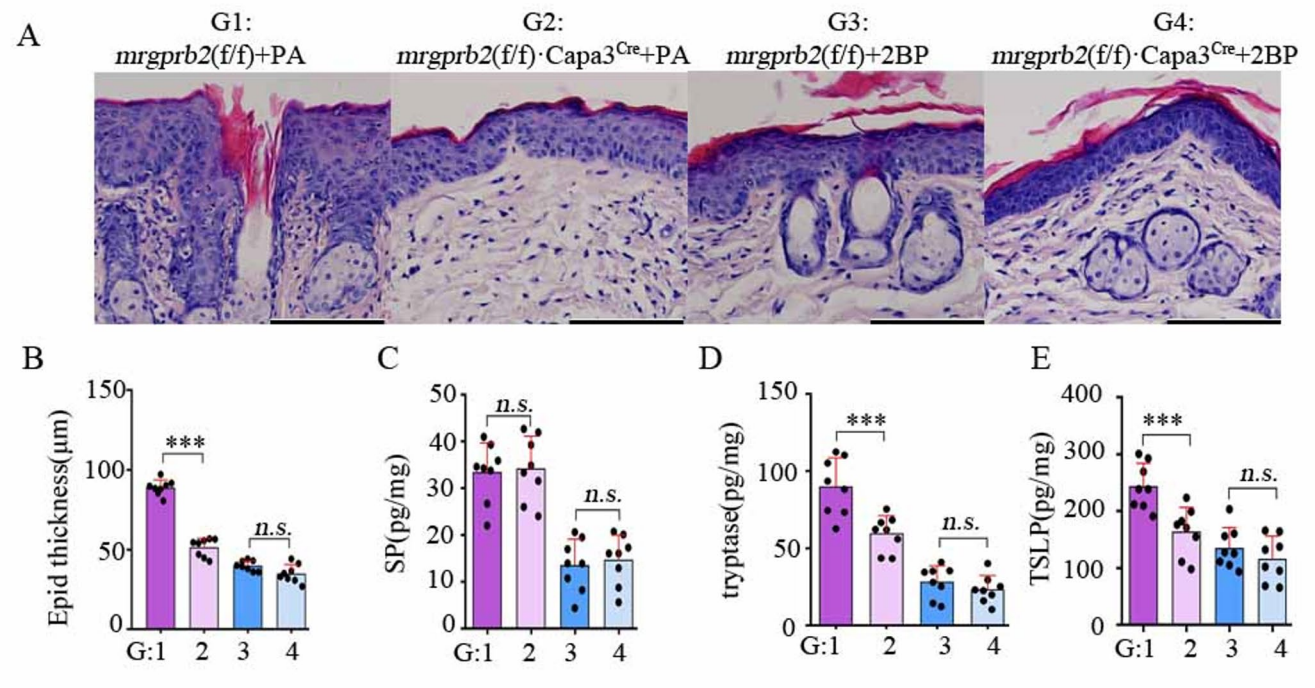

Fig. 3 Role of MCs-specific MRGPRB2 in MC903/PA- or MC903/2BP-induced dermatitis. MC903 was topically applied to the exposed nape of 8–10-week-old *mrgprb2*(f/f)·Capa3^{Cre} mice and *mrgprb2*(f/f) mice for 12 consecutive days. On days 3, 6, 9, the mice received intradermal injection of PA (2 μg/cm^2) or 2BP (2 μg/cm^2). **A** HE staining of the skin lesions (scale bar = 100 μm), **B** epidermal(Epid) thickness, **C** skin SP, **D** skin tryptase and **E** skin TSLP are shown. Statistics: One-way ANOVA + Bonferroni's tests, ***$P < 0.001$, n.s. $P > 0.05$

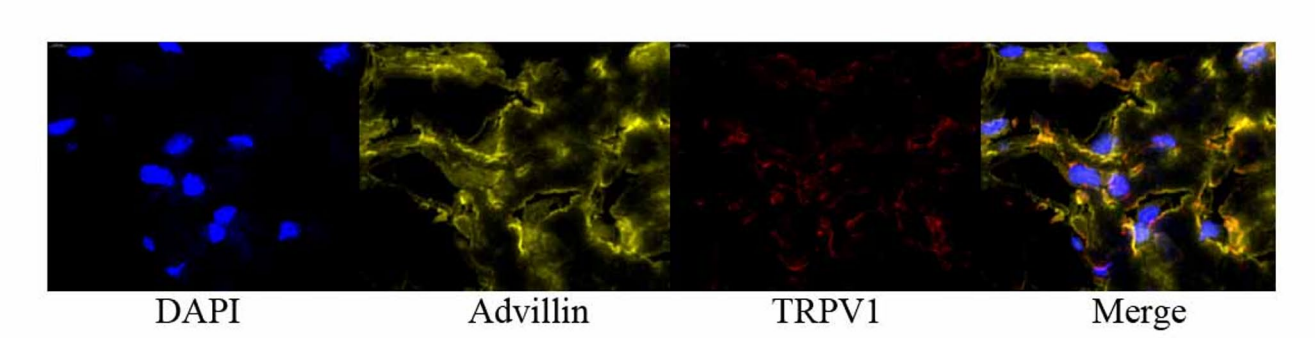

Fig. 4 Skin lesions from AD mice were stained with anti-Advillin and anti-TRPV1. Immunofluorescence displays their expressions and co-localization in the dermis

PA or 2BP. Figure 5C showed that these levels remained unchanged in the MC903 or MC903 + 2BP groups, and were only slightly upregulated in the MC903 + PA group compared with that in the MC903 group. In contrast, SCMK significantly increased these levels; the addition of PA or 2BP further increased or conversely reduced TRPV1 S-palmitoylation along with supernatant SP level, respectively, without affecting SGK1 and NEDD4L phosphorylation (Fig. 5D). Compared with DRGs from *nedd4l*(f/f) mice, SCMK increased levels of total and S-palmitoylated TRPV1 and supernatant SP without affecting SGK1 phosphorylation in DRGs from *nedd4l*(f/f)·Advillin^{Cre} mice; the addition of PA or 2BP further increased or conversely reduced TRPV1 S-palmitoylation and supernatant SP levels in the latter DRGs, respectively, without affecting total TRPV1 levels (Fig. 5E). Compared to the DRGs isolated from *sgk1*(f/-) mice, the DRGs isolated from *sgk1*(f/-)·Advillin^{Cre} mice (Fig. 5F) exhibited slight or marked reductions in total and S-palmitoylated TRPV1 and supernatant SP following SCMK or SCMK + PA treatment, respectively; these levels were also markedly reduced by SCMK + 2BP, except for total TRPV1. The undetectable TRPV1 S-palmitoylation in the SCMK + PA group may be the result from lysosomal degradation of TRPV1. As expected, the addition of lysosome inhibitor BafA1 to SCMK + PA significantly up-regulated the levels of total and S-palmitoylated TRPV1 and supernatant SP (Fig. 5G). Figure 5E, F also confirmed the knockdown of NEDD4L or SGK1 in DRGs from *nedd4l*(f/f)·Advillin^{Cre} or *sgk1*(f/-)·Advillin^{Cre} mice, respectively, and showed that SGK1 knockdown limits NEDD4L phosphorylation. Collectively, these data suggest that TRPV1 S-palmitoylation is required for SP production but also facilitates lysosomal degradation of TRPV1 with involvement of NEDD4L in DRGs; however, under SCMK treatment, NEDD4L activity in *wt* DRGs is inhibited by high levels of phosphorylated SGK1, thereby maintaining TRPV1 abundance and SP production.

SGK1/NEDD4L signalling in sensory nerves contributing to SP production and AD severity

Under MC903 exposure, compared with *nedd4l*(f/f) mice, increases in skin SP, tryptase, TSLP, and epidermal thickness were observed in *nedd4l*(f/f)·Advillin^{Cre} mice; these increases were further significantly exacerbated by addition of intradermal injection of PA and were attenuated by 2BP (Fig. 6A–E). Under MC903 exposure, compared with *sgk1*(f/-) mice, although no statistically significant differences were detected, slight reductions in skin SP, tryptase, TSLP, and epidermal thickness were observed in *sgk1*(f/-)·Advillin^{Cre} mice; however, these reductions were further exacerbated by intradermal injection of PA or 2BP. In *sgk1*(f/-)·Advillin^{Cre} mice treated with MC903 + PA, supplementation with intradermal SP significantly upregulated skin tryptase, TSLP, and epidermal thickness; however, in *sgk1*(f/-)·Advillin^{Cre} mice treated with MC903 + 2BP, intradermal SP supplementation failed to alter skin tryptase, TSLP or epidermal thickness (Fig. 6F–J).

Palmitoylation suppresses NEDD4L-mediated MRGPRB2 reduction and promotes tryptase release in mBMMCs

Using the alphafold3 software for protein–protein docking, mouse NEDD4L and MRGPRB2 were shown to interact closely, with a binding free energy of -−19.4 kcal/mol and multiple hydrogen bonding at different interface(Fig. 7A). Currently, a commercially available antibody against MRGPRB2 is not available. Therefore, a plasmid expressing MRGPRB2 with a Flag tag at the C-terminus (MRGPRB2·Flag) was overexpressed in mature mBMMCs isolated from *mrgprb2*(f/f)·Cmv^{Cre} mice, *mrgprb2*(f/f)/*nedd4l*(f/f)·Cmv^{Cre} or *mrgprb2*(f/f)/*sgk1*(f/f)·Cmv^{Cre} mice. CO-IP assay(Fig. 7B) demonstrated a physical interaction between NEDD4L and MRGPRB2·Flag or SGK1

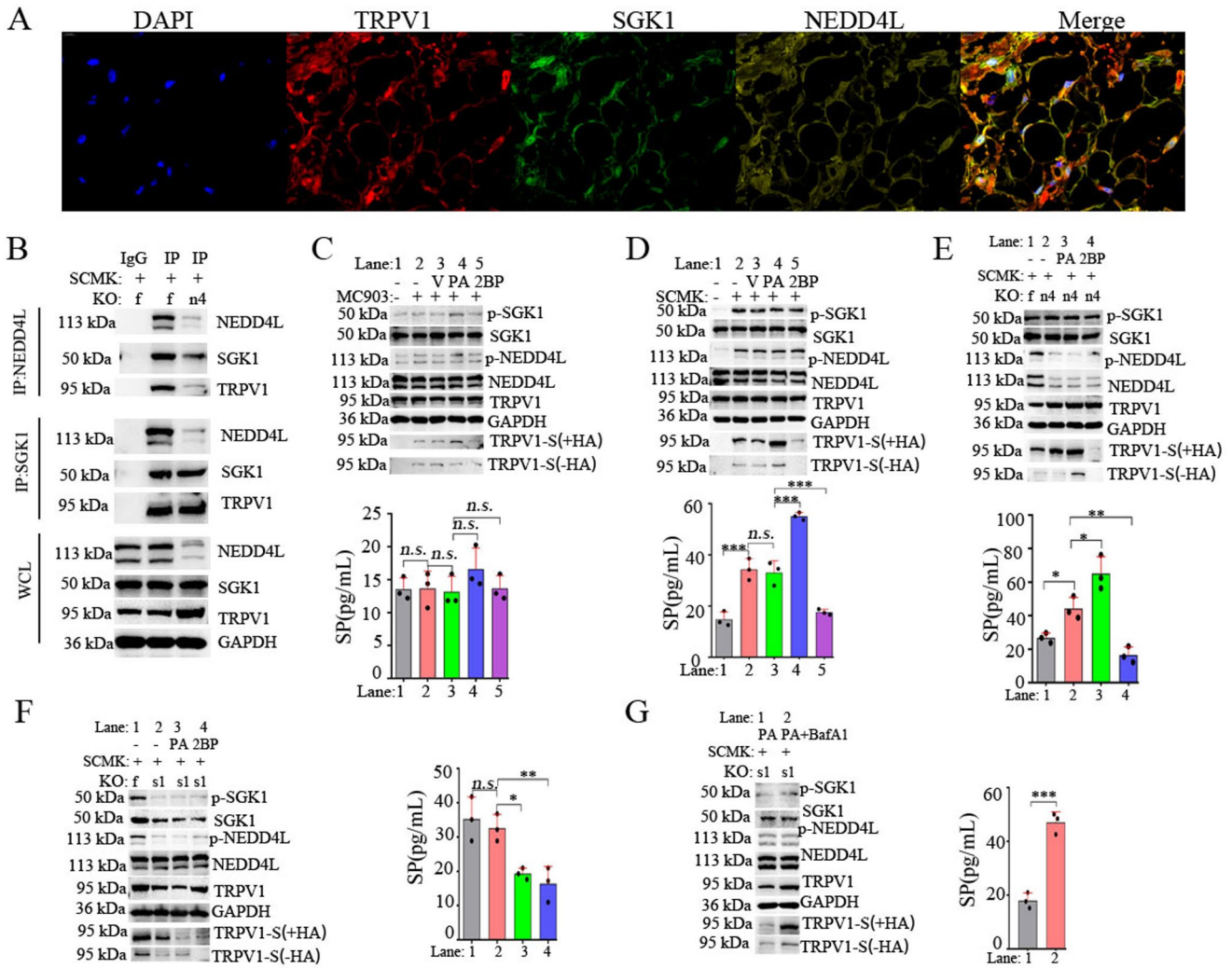

Fig. 5 SGK1/NEDD4L pathway regulating TRPV1 S-palmitoylation and SP expression in DRGs in vitro. Skin lesions from *wt* AD mice were stained with anti-TRPV1, SGK1 and NEDD4L, and immunofluorescence displays their expressions and co-localization in the dermis **A**. DRGs isolated from *nedd4l*(f/f) mice(f) and *nedd4l*(f/f)·Advillin^{Cre} mice(n4) were cultured *in vitro* and stimulated with supernatants collected from MC903-treated keratinocytes(SCMK) for 30 h, and then immunoprecipitation of DRGs lysates was performed using anti-NEDD4L and anti-SGK1, respectively, followed by western blotting **B**. DRGs isolated from *wt* mice were cultured in vitro and stimulated with MC903(100 ng/mL)±PA (100 μM) or ±2BP (20 μM) for 30 h **C**. DRGs isolated from *wt* mice were cultured in vitro and stimulated with SCMK±PA (100 μM) or ±2BP (20 μM) for 30 h **D**. DRGs isolated from *nedd4l*(f/f) and *nedd4l*(f/f)·Advillin^{Cre} mice were cultured *in vitro* and stimulated with SCMK±PA (100 μM) or ±2BP (20 μM) for 30 h **E**. DRGs isolated from *sgk1*(f/-) mice(f) and *sgk1*(f/-)·Advillin^{Cre} mice(s1) were cultured in vitro and stimulated with SCMK±PA (100 μM) or ±2BP (20 μM) for 30 h **F**. DRGs isolated from *sgk1*(f/-)·Advillin^{Cre} mice were cultured in vitro and stimulated with SCMK+PA (100 μM)±BafA1(30 nM) for 30 h **G**. The indicated levels of protein in DRGs and SP in supernatants were determined. Statistics: One-way ANOVA+Bonferroni's tests, $^{*}P<0.05$, $^{**}P<0.01$, $^{***}P<0.001$, n.s. $P>0.05$

in mBMMCs, while MRGPRB2·Flag and SGK1 were not detected in immunoprecipitates obtained with anti-NEDD4L following *nedd4l* KO; moreover, *nedd4l* KO significantly abolished the presence of MRGPRB2·Flag in immunoprecipitates obtained with anti-SGK1, suggesting that NEDD4L may act as a scaffold facilitating the interaction between SGK1 and MRGPRB2·Flag in mBMMCs.

Subsequently, mBMMCs overexpressing MRGPRB2·Flag were treated with SP, SP+PA or SP+2BP. SP slightly increased SGK1 and NEDD4L phosphorylation and significantly induced MRGPRB2·Flag S-palmitoylation and tryptase release, without affecting the levels of total SGK1,NEDD4L, or MRGPRB2·Flag(Fig. 7C). The addition of PA or 2BP did not alter SGK1 and NEDD4L phosphorylation. Total and S-palmitoylated MRGPRB2·Flag levels, as well as tryptase release, were further upregulated by PA addition, whereas they were markedly reduced by 2BP addition. In MRGPRB2·Flag-overexpressing mBMMCs treated with SP, *nedd4l* KO mildly upregulated total and S-palmitoylated MRGPRB2·Flag without affecting total

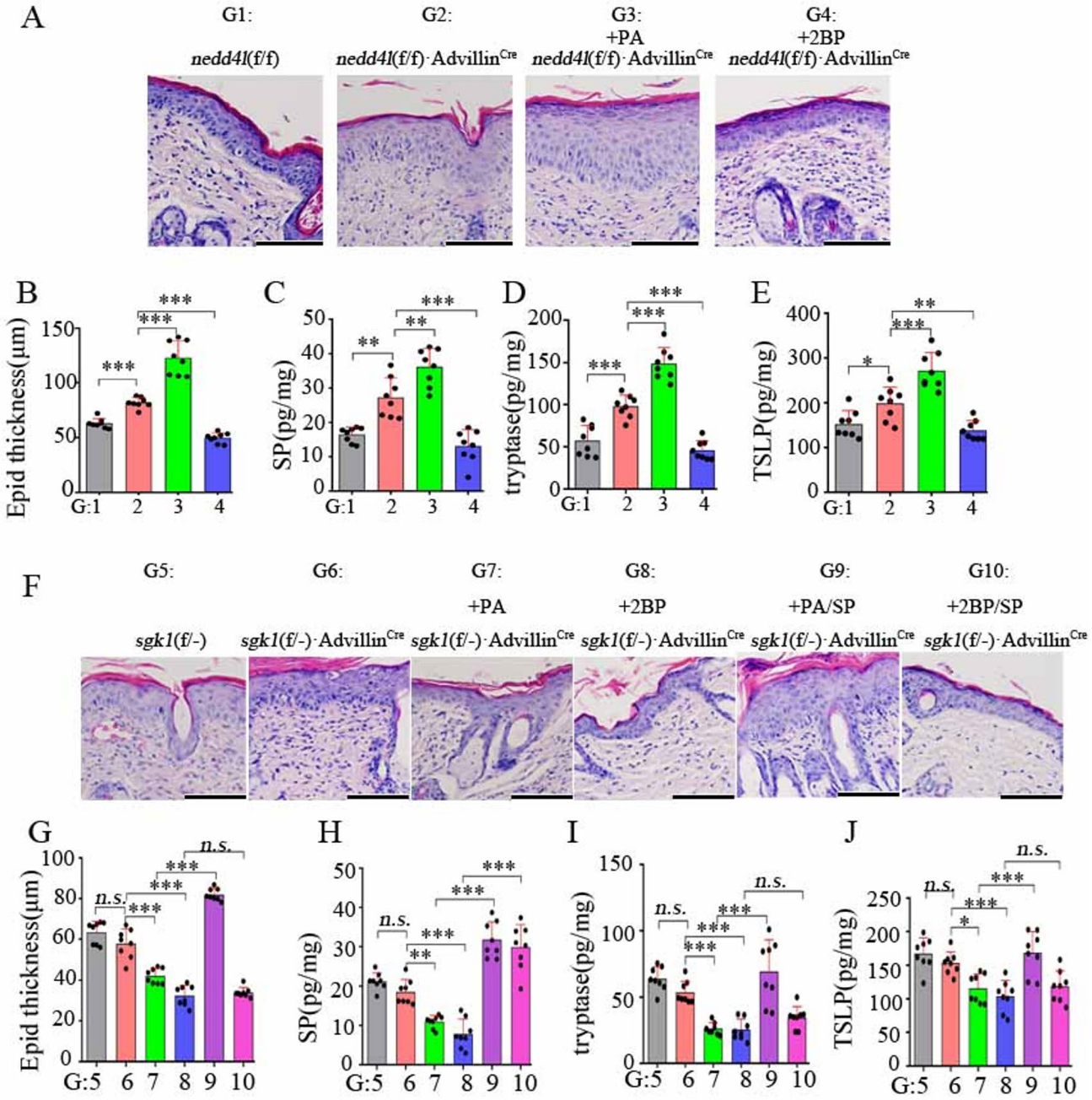

Fig. 6 The effect of SGK1/NEDD4L signalling in sensory nerves on AD severity in mice. MC903 was topically applied to the exposed nape of 8–10-week-old *nedd4l*(f/f) and *nedd4l*(f/f)·Advillin^{Cre} mice for 12 consecutive days. On days 3, 6, 9, the *nedd4l*(f/f)·Advillin^{Cre} mice received intradermal injection of PA (2 μg/cm^2), or 2BP(2 μg/cm^2). **A** HE staining of the skin lesions (scale bar = 100 μm), **B** epidermal (Epid) thickness, **C** skin SP, **D** skin tryptase, **E** skin TSLP are shown. In addition, MC903 was topically applied to the exposed nape of 8–10-week-old *sgkl*(f/-) and *sgk1*(f/-)·Advillin^{Cre} mice for 12 consecutive days. On days 3, 6, 9, *sgk1*(f/-)·Advillin^{Cre} mice received intradermal injection of PA (2 μg/cm^2), PA + SP (10 ng/cm^2), 2BP (2 μg/cm^2), or 2BP + SP (10 ng/cm^2). **F** HE staining of the skin lesions (scale bar = 100 μm), **G** epidermal(Epid) thickness, **H** skin SP, **I** skin tryptase, **J** skin TSLP are shown. Epid, epidermal. Statistics: One-way ANOVA + Bonferroni's tests, *$P < 0.05$, **$P < 0.01$, ***$P < 0.001$, n.s. $P > 0.05$

and phosphorylated SGK1. The addition of PA or 2BP did not change total MRGPRB2·Flag levels; however, MRGPRB2·Flag S-palmitoylation and tryptase release were significantly upregulated by PA addition and markedly suppressed by 2BP in mBMMCs with *nedd4l* KO(Fig. 7D). In MRGPRB2·Flag-overexpressing mBMMCs treated with SP, *sgk1* KO blocked NEDD4L phosphorylation without affecting the levels of total and S-palmitoylated

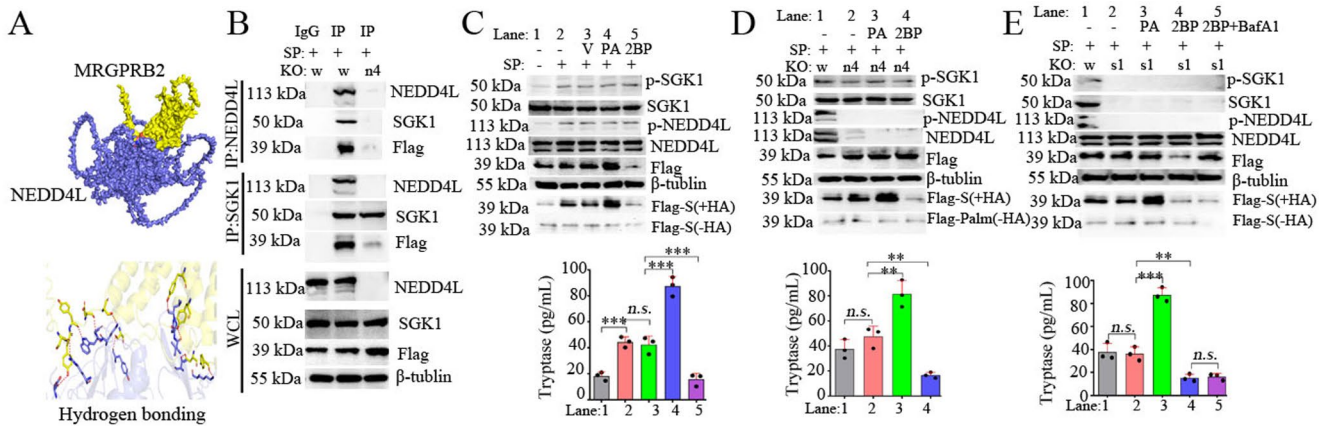

Fig. 7 SGK1/NEDD4L pathway regulating MRGPRB2 S-palmitoylation and tryptase releasing in mBMMCs in vitro. Using software alphafold3 for the molecular docking of mouse NEDD4L and MRGPRB2 proteins, the structure and hydrogen bonding are shown **A**. We induced differentiation of marrow cells isolated from adult *mrgprb2*(f/f)·Cmv^{Cre} mice (w) and *mrgprb2*(f/f)/*nedd4l*(f/f)·Cmv^{Cre} mice (n4) into mBMMCs by in vitro culture. mBMMCs were then transfected with plasmid-expressing MRGPRB2·Flag and 24 h later, the cells were stimulated with SP (30 μM) for 24 h. Immunoprecipitation of mBMMCs lysates was performed using anti-NEDD4L and anti-SGK1, respectively, followed by western blotting **B**. mBMMCs derived from adult *mrgprb2*(f/f)·Cmv^{Cre} mice were transfected with plasmid-expressing MRGPRB2·Flag. After 24 h, the cells were stimulated with SP (30 μM), SP+PA (100 μM) or SP+2BP (20 μM) for 24 h **C**. mBMMCs derived from adult *mrgprb2*(f/f)·Cmv^{Cre} mice (w), *mrgprb2*(f/f)/*nedd4l*(f/f)·Cmv^{Cre} mice (n4, **D**) and *mrgprb2*(f/f)/*sgk1*(f/f)·Cmv^{Cre} mice (s1, **E**) were transfected with plasmid-expressing MRGPRB2·Flag. After 24 h, the cells were stimulated with SP (30 μM), SP+PA, SP+2BP or SP+BafA1(30 nM, **E**) for 24 h. The indicated levels of protein in mBMMCs and tryptase level in supernatants were determined. Statistics: One-way ANOVA+Bonferroni's tests, $*P<0.05$, $**P<0.01$, $***P<0.001$, n.s. $P>0.05$

MRGPRB2·Flag or tryptase release; the addition of PA further enhanced MRGPRB2·Flag S-palmitoylation and tryptase release without affecting total MRGPRB2·Flag levels. In contrast, the addition of 2BP markedly reduced the levels of total and S-palmitoylated MRGPRB2·Flag and tryptase release, whereas co-treatment with 2BP plus BafA1 (a lysosome inhibitor) restored total MRGPRB2·Flag without affecting MRGPRB2·Flag S-palmitoylation or tryptase release compared with that via 2BP treatment alone. (Fig. 7E). These data indicate that MRGPRB2 S-palmitoylation promotes tryptase release in BMMCs and also inhibits NEDD4L-mediated lysosomal degradation of MRGPRB2, despite high NEDD4L activity resulting from low levels of phosphorylated SGK1 under SP treatment.

SGK1/NEDD4L signalling in MCs orchestrating tryptase release and AD severity

Under MC903 exposure, no significant differences in skin SP, tryptase, TSLP, and epidermal thickness were observed among *nedd4l*(f/f) mice, *nedd4l*(f/f)·Capa3^{Cre} mice and *nedd4l*(f/f)/*sgk1*(f/f)·Capa3^{Cre} mice (Fig. 8A–E). In MC903-treated *nedd4l*(f/f)·Capa3^{Cre} mice, skin SP, tryptase, TSLP, and epidermal thickness were all markedly upregulated by intradermal injection of PA and were all downregulated by the 2BP compared with that in the control group (Fig. 8A–E). There were no significant differences in skin SP, tryptase, TSLP, and epidermal thickness between MC903-treated *sgk1*(f/f) mice and *sgk1*(f/f)·Capa3^{Cre} mice (Fig. 8F, G). In MC903-treated *sgk1*(f/f)·Capa3^{Cre} mice, PA addition intensified skin SP, tryptase, TSLP expression, and epidermal thickness to a similar same extent; in contrast, 2BP addition markedly reduced these parameters. Notably, intradermal SP supplementation did not increase skin tryptase or TSLP levels or epidermal thickness in MC903-treated *sgk1*(f/f)·Capa3^{Cre} mice receiving concomitant 2BP administration, further suggesting that the effect of SP is antagonised by 2BP.

Discussion

Epidermal barrier function can be impaired or restored by skin fatty acids when the relative abundance of specific components changed [38]. Van Smeden et al. found that stratum C16:0 (PA) and C18:0 contents were increased in both skin lesions and non-lesions of AD patients; however, the more pronounced increase in lesions may contribute to skin lipid re-organization and reduced barrier function [32, 39]. However, Li et al. recently demonstrated a significant decrease in PA, C18:0 and C18:2n6 in the posterior neck lesions from AD patients compared with that from non-AD controls [40]. Similarly, the present study provided previously unreported evidence that there was an increase in PA, C16:1, and C18:1n9c in lesional skin from the nape-AD model, and increase in PA, C18:0, C18:1n9t, C20:1, C20:4n6, and C22:6n3 in lesional skin from the ear-AD model. Moreover, the increase in skin PA was markedly

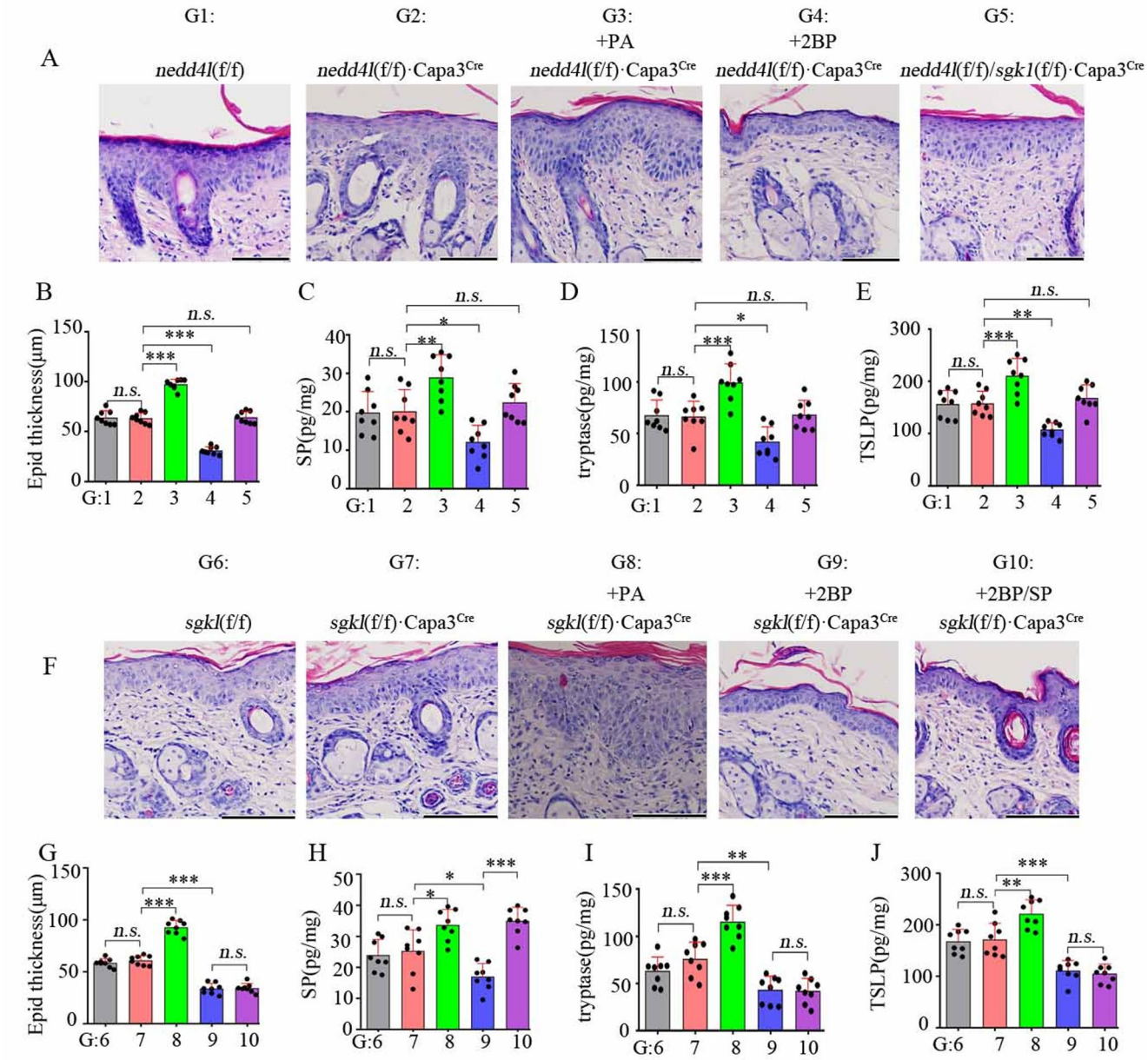

Fig. 8 The effect of SGK1/NEDD4L signalling in MCs on AD severity in mice. MC903 was topically applied to the exposed nape of 8–10-week-old *nedd4l*(f/f), *nedd4l*(f/f)·Capa3^{Cre}, *nedd4l*(f/f)/*sgk1*(f/f)·Capa3^{Cre} mice for 12 consecutive days. On days 3, 6, 9, the *nedd4l*(f/f)·Capa3^{Cre} mice received intradermal injection of PA (2 μg/cm^2), or 2BP (2 μg/cm^2). **A** HE staining of the skin lesions (scale bar = 100 μm), **B** epidermal(Epid) thickness, **C** skin SP, **D** skin tryptase, **E** skin TSLP are shown. In addition, MC903 was topically applied to the exposed nape of 8–10-week-old *sgkl*(f/f) and *sgk1*(f/f)·Capa3^{Cre} mice for 12 consecutive days. On days 3, 6, 9, *sgk1*(f/f)·Capa3^{Cre} mice received intradermal injection of PA (2 μg/cm^2), 2BP (2 μg/cm^2), or 2BP + SP (10 ng/cm^2). **F** HE staining of the skin lesions (scale bar = 100 μm), **G** epidermal(Epid) thickness, **H** skin SP, **I** skin tryptase, **J** skin TSLP are shown. Statistics: One-way ANOVA + Bonferroni's tests, *$P < 0.05$, **$P < 0.01$, ***$P < 0.001$, n.s. $P > 0.05$

greater in the nape than the ear. This difference may be attributable to the adipose-rich nature of the nape, whereas the ear is predominantly composed of cartilage. In addition, possibly owing to richer microcirculation and higher transdermal absorption of MC903 in the ear, substantially higher levels of lesional SP, tryptase, TSLP, and IL-13 were observed in ear-AD compared with that in nape-AD model. Interestingly, non-specific inflammation (characterised by increased IL-1β, IL-6 and TNF-α) and up-regulation of several ML-CFAs (including PA, C18:0, C18:1n9t, C20:1, and C22:6n3) in spinal cord were observed in nape-AD but not in ear-AD models. This difference may be related to the close

anatomical proximity of nape lesions to the spinal cord. In this regard, identifying differences in neuroinflammatory responses arising from anatomical variation between the two AD models is essential for selecting appropriate models for specific research purposes.

Yang et al. recently demonstrated that spinal PA promotes nape-AD through spinal TRPV1 and MRGPRD signaling, with concomitant increases in itch-related gene expressions in DRGs [36]. More recently, Kim et al. found higher PA level in skin lesions colonised with methicillin-resistant S. aureus (MRSA) than in the skin lesions without MRSA colonization from AD patients [41]. The role of excessive skin PA production in AD can be partially explained in obesity-mediated exacerbation of AD in mice. They showed that skin CD36-sterol-regulatory element binding protein1 (SREBP1)-related fatty acid accumulation and circulation PA levels are markedly increased by a high-fat diet, and that keratinocyte-derived TSLP expression is also increased by PA treatment in vitro via CD36-SREBP1 signaling pathway [42]. However, the role of PA-promoted protein S-palmitoylation in obesity-mediated AD exacerbation was not addressed. In the nape- and ear-AD models used in this study, the epidermal thickness was aggravated and alleviated by intradermal injection of PA and 2BP, respectively, along with consistent changes in skin SP, tryptase, TSLP, and IL-13, and spinal GRP. The effect of 2BP is likely attributable to its antagonism of protein S-palmitoylation resulting from MC903-induced endogenous PA elevation. Alterations in spinal GRP are associated with the severity of chronic pruritus during AD development. In addition, neither the addition of PA nor 2BP affected total serum IgE levels in either AD model. However, Segawa et al. found that ovalbumin chemically coupled with PA failed to induce anti-ovalbumin IgE antibody without affecting IgG antibody production in BALB/c male mice [43]; this effect depends on the alteration in antigen structure, which is unlikely to occur in the present AD models.

SP–tryptase–Th2 inflammation axis is well characterised in AD, and SP is mainly produced by TRPV1$^+$ sensory nerve [25]; we also confirmed that subcutaneous injection of the TRPV1 antagonist capsazepine could partially reduce skin SP up-regulation and epidermal thickening in AD-like mice. Therefore, skin SP production is likely to represent an upstream factor in AD phenotype alterations induced by S-palmitoylation intervention. Evidence showing that TRPV1$^+$ nociceptor ablation suppresses skin SP and concomitantly reduces skin tryptase and TSLP, and epidermal thickness, whereas SP supplementation reverses the phenotype and the addition of a tryptase inhibitor antagonises the effects of SP by reducing skin TSLP, supports the hypothesis. Interestingly, the addition of 2BP antagonised the effects of SP on the AD phenotype by reducing skin tryptase, suggesting that inhibiting skin S-palmitoylation leading to AD alleviation may also be related to suppressing SP-mediated MCs degranulation. The role of MCs-specific MRGPRB2 in AD has been reported [25]. The current study further demonstrated that cKO of *mrgprb2* in MCs significantly decreased skin tryptase, TSLP, and epidermal thickness without affecting skin SP under MC903 + PA treatment, suggesting that PA-mediated AD exacerbation partially relies on MRGPRB2 signaling in MCs in addition to the up-regulation of SP production. In contrast, *mrgprb2* cKO had no notable effect under MC903 + 2BP treatment, indicating that deleting *mrgprb2* in MCs cannot further alleviate AD severity under 2BP treatment, possibly owing to reduced upstream SP. In addition, previous studies have shown that skin TSLP originates from keratinocytes in MC903-induced AD-like mice [44], and in vitro experiments have further confirmed that MC903 can stimulate keratinocytes to produce TSLP [45]. The present study demonstrated that the TRPV1$^+$ nociceptor–SP–MCs MRGPRB2–tryptase axis, one of the targets of skin PA, markedly promotes skin TSLP production in an MC903-induced murine AD model; however, this does not rule out the possibility that PA can facilitate MC903-induced TSLP production by keratinocytes in vitro.

Instead, it was found that the total and S-palmitoylated TRPV1 protein levels, as well as SP production in DRGs in in vitro studies, cannot be directly influenced by MC903, MC903 + PA or MC903 + 2BP. However, TRPV1 S-palmitoylation and SP production in DRGs were up-regulated by SCMK, and they were further aggravated by the addition of PA but mitigated by 2BP, which is consistent with findings from the in vivo studies. This supports a previously unsubstantiated speculation that skin SP production in AD models is secondary to MC903-induced keratinocytes stimulation and is regulated by TRPV1 S-palmitoylation in sensory nerves. As expected, SP administration induced tryptase release in mBMMCs and simultaneously induced MRGPRB2 S-palmitoylation. Interestingly, this phenomenon was aggravated by PA (along with upregulation of total MRGPRB2) and attenuated by 2BP (along with reduction in total MRGPRB2). This represents a novel and important finding for understanding the SP- MRGPRB2-tryptase axis. These data suggest that, within skin neuro-immune cross-talk in AD, TRPV1 S-palmitoylation in sensory nerves and MRGPRB2 S-palmitoylation in MCs synergistically promote AD by enhancing SP production and releasing tryptase, respectively.

SGK1/NEDD4L signalling may regulate the biological activity of TRPV1$^+$ sensory nerves and MCs, as described in the introduction. In the current study, conclusive evidence was provided that dermal TRPV1 protein is colocalised with SGK1 and NEDD4L, that TRPV1 physically interacts with

SGK1 and NEDD4L in DRGs, and that NEDD4L physically interacts with MRGPRB2 in primary mBMMCs. Therefore, the roles of SGK1/NEDD4L signalling in sensory nerves or MCs during AD development were determined both in vivo and in vitro. The expression and function of NEDD4L in DRGs or nociceptors were preliminarily explored. In neuropathic pain, sensory neuron voltage-gated sodium channels ($Na_v1.7$) and high-voltage-activated calcium channels (HVACCs) are finely regulated by the E3 ligase activity of NEDD4L [46, 47]. Moreover, NEDD4L interacts with TRPA1 and thereby mediates it ubiquitination in mouse DRGs [48]. Yu et al. showed that *nedd4l* depletion in neurons enhances TrkA receptor protein stability and increases the number of skin SP-positive neurons [49]. Here, it was found that the MC903–SP–tryptase–TSLP–AD axis was enhanced or impaired following *nedd4l* or *sgk1* KO in sensory nerves through modulation of skin SP production, respectively. Mechanistically, total and S-palmitoylated TRPV1 levels and SP production in DRGs isolated from mice with *nedd4l* or *sgk1* KO in sensory nerves were up-regulated and down-regulated by SCMK, respectively. These data suggest that non-phosphorylated NEDD4L directly down-regulates TRPV1 protein in DRGs or sensory nerves. He et al. showed that TRPV1 is a direct target of SGK1, as demonstrated by co-immunoprecipitation, and that *sgk1* knockdown reduces TRPV1 expression in mouse bladder smooth muscle cells [22], further supporting these findings. In addition, several research groups have extensively explored the role of SGK1/NEDD4L in IgE-mediated MCs degranulation and bacterial DNA-induced inflammation response in MCs [5, 13, 50, 51]; however, none of these studies involved the tryptase release. This study provided new evidence that MC903-SP-tryptase-TSLP-AD axis is not affected by *nedd4l* or *sgk1* cKO in MCs *in vivo*. Similarly, MRGPRB2 S-palmitoylation and tryptase release were also not influenced by *nedd4l* or *sgk1* KO in SP-treated mBMMCs, whereas total MRGPRB2 abundance was up-regulated following *nedd4l* KO.

The above analysis speculates that the S-palmitoylation is highly likely to be a regulatory factor involved in maintaining the protein abundance of TRPV1 and MRGPRB2, which is orchestrated by SGK1/NEDD4L signaling. Further evidence clearly showed that, in mice with *nedd4l* cKO in sensory nerves, intradermal injection of PA and 2BP aggravated and attenuated skin SP production, respectively, alongside consistent changes in tryptase-TSLP-AD axis. In contrast, skin SP production and the downstream axis were blocked by both PA and 2BP in mice with *sgk1* cKO in sensory nerves; however, SP supplementation reversed the tryptase-TSLP-AD axis only in the PA group but not in the 2BP group. Mechanistically, under SCMK treatment, TRPV1 S-palmitoylation and SP production were up-regulated by PA but down-regulated by 2BP in *nedd4l* knockdown DRGs, whereas both parameters were down-regulated by PA or 2BP in *sgk1* knockdown DRGs. Moreover, PA significantly accelerated and 2BP blocked TRPV1 protein reduction in *sgk1* knockdown DRGs; additionally, the inclusion of a lysosome inhibitor in PA-treated group antagonised the reductions in total and S-palmitoylated TRPV1 levels and SP production. Collectively, these data demonstrate that TRPV1 S-palmitoylation in sensory nerves is beneficial for SP production; however, TRPV1 is more readily degraded in lysosomes when NEDD4L is not phosphorylated by SGK1(NEDD4L is phosphorylated by SGK1 in DRGs under SCMK treatment), a mechanism partially suggested by a previous study [21].

A factual consideration must be noted: intradermal injections of PA or 2BP also affect MRGPRB2 in MCs. In mice with *nedd4l* or *sgk1* cKO in MCs, tryptase–TSLP–AD axis was enhanced by PA and that was attenuated by 2BP. However, the observed increases or decreases in skin SP production may also have contributed to these outcomes, as *nedd4l* or *sgk1* were not modified in sensory nerves. Furthermore, SP supplementation failed to induce an increase in skin tryptase levels in mice with *sgk1* cKO in MCs treated with 2BP, suggesting an inhibitory effect of 2BP on MRGPRB2 S-palmitoylation; this mechanism may also be present in mice with *sgk1* cKO in sensory nerves treated with 2BP + SP. In vitro experiments using mBMMCs further highlighted the mechanistic complexity. PA prompted while 2BP inhibited SP-mediated MRGPRB2 S-palmitoylation and tryptase release following *nedd4l* or *sgk1* deletion. However, total MRGPRB2 levels were significantly reduced in mBMMCs with *sgk1* deletion under 2BP + SP treatment, and the addition of a lysosome inhibitor prevented MRGPRB2 reduction without affecting MRGPRB2 S-palmitoylation and tryptase release. Collectively, these data show that S-palmitoylated MRGPRB2 in MCs resists being sorted into NEDD4L-mediated lysosomal degradation, despite elevated NEDD4L activity resulting from low levels of phosphorylated SGK1 under SP stimulation, thereby favoring SP-mediated tryptase release.

Limitations

Several limitations of this study cannot be ignored. First, the mechanism underlying skin PA increases in AD-like lesions, as well as the biological significance of alterations in skin ML-CFAs other than PA in AD, remains to be explored. Second, the enzymes responsible for the S-palmitoylation of TRPV1 in sensory nerves and MRGPRB2 in MCs were not further elucidated experimentally. Third, confirmation of interactions between non-phosphorylated NEDD4L and TRPV1 or MRGPRB2, as well as its role in mediating

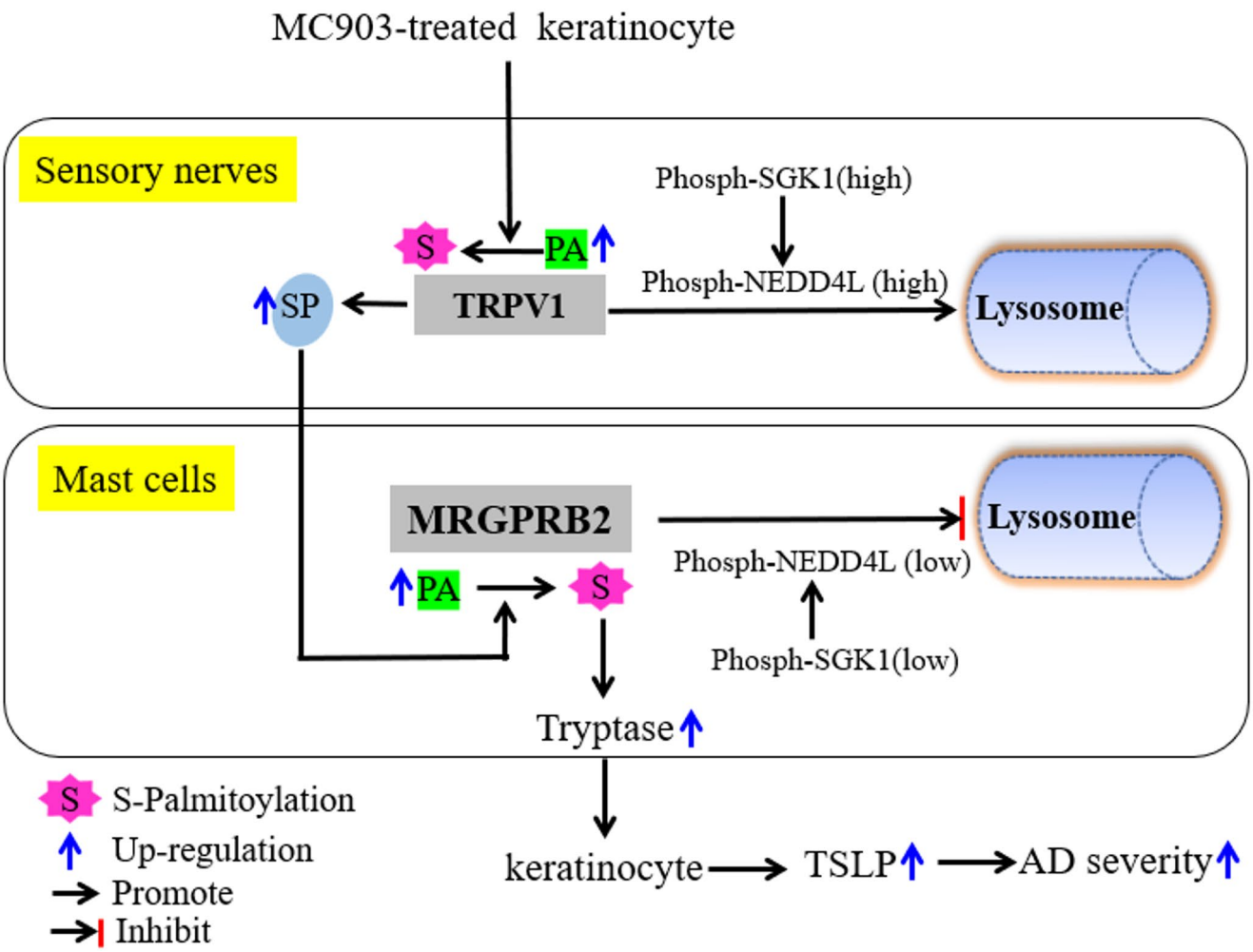

Fig. 9 PA intensifies TRPV1$^+$ nociceptor-SP-MCs MRGPRB2-tryptase axis in AD mice via driving S-palmitoylation of TRPV1 and MRGPRB2

their ubiquitination using yeast two-hybridization or GST pull-down assays in vitro, would provide more convincing evidence for these findings. Fourth, given the complexity of skin neuro-immune interactions, inflammatory mediators released from MC903-treated keratinocytes may also directly affect the function of MRGPRB2-expressing MCs independently of SP. Fifth, the optimal concentrations of the chemical reagents used, including PA, SP, Ben, and BafA1, were not determined through assessment of their dose-dependent effects. Lastly, although MC903 is widely used to induce AD-like dermatitis in mice, vitamin D receptor stimulation does not induce dermatitis in humans but instead represents a therapeutic approach for psoriasis [52], a condition that shares several similarities with AD; moreover, murine AD models do not fully recapitulate human AD pathology and may share only certain mechanistic features.

Conclusions

Altogether, this study demonstrates that PA in skin lesions are significantly up-regulated in the nape- and ear-AD murine models induced by topical MC903, and intradermal injection of PA remarkably aggravates AD by enhancing TRPV1$^+$ nociceptor–SP–MCs MRGPRB2–tryptase axis. Specifically, following exposure to supernatants collected from MC903-treated keratinocytes, PA promotes TRPV1 S-palmitoylation and SP production in DRGs, while S-palmitoylated TRPV1 is easily degraded by NEDD4L-involved lysosomal pathways; however, NEDD4L activity in DRGs is inhibited by high levels of phosphorylated SGK1. Under SP treatment, PA similarly promotes MRGPRB2 S-palmitoylation and tryptase release in MCs; however, S-palmitoylated MRGPRB2 resists being sorted into NEDD4L-mediated lysosomal degradation, despite elevated NEDD4L activity resulting from low levels of phosphorylated SGK1 (Fig. 9).

Supplementary Information The online version contains supplementary material available at https://doi.org/10.1007/s00011-026-02184-y.

Acknowledgements None.

Author contributions JY, FH and ZY: study design, conceptualization, methodology, supervision and revision of the manuscript. TS and WW: original manuscript writing. BC: funding acquisition, investigation, data processing, original manuscript writing and manuscript editing.

Funding This work was supported by grants from National Natural Science Foundation of China (82373479), Medical youth top-talent project in Chongqing (YXQN202462) and Funding for Postdoctoral Fellowships in Chongqing (55012).

Data availability The data supporting the findings of this study are available from the corresponding author upon reasonable request.

Declarations

Conflict of interest The authors declare no conflict of interest.

Ethical approval The animal experiments and executions in this study were approved by the Ethics Committee of Chongqing University Three Gorges Hospital.

Consent for publication All authors have read and agreed with the submission of the manuscript to Inflammation Research.

References

1. Tian J, Zhang D, Yang Y, et al. Global epidemiology of atopic dermatitis: a comprehensive systematic analysis and modelling study. Br J Dermatol. 2023;190(1):55–61.
2. Brabenec L, Gupta S, Eichwald T, et al. Decoding the neuroimmune axis in the atopic march: mechanisms and implications. Curr Opin Immunol. 2024;91:102507.
3. Steinhoff M, Ahmad F, Pandey A, et al. Neuroimmune communication regulating pruritus in atopic dermatitis. J Allergy Clin Immunol. 2022;149(6):1875–98.
4. Tsagareli MG, Follansbee T, Iodi Carstens M, et al. Targeting transient receptor potential (TRP) channels, mas-related G-protein-coupled receptors (Mrgprs), and protease-activated receptors (PARs) to relieve itch. Pharmaceuticals (Basel). 2023;16(12):1707.
5. Yip KH, Kolesnikoff N, Hauschild N, et al. The Nedd4-2/Ndfip1 axis is a negative regulator of IgE-mediated mast cell activation. Nat Commun. 2016;7:13198.
6. Gao S, Alarcón C, Sapkota G, et al. Ubiquitin ligase Nedd4L targets activated Smad2/3 to limit TGF-beta signaling. Mol Cell. 2009;36(3):457–68.
7. Dong C, Lin JM, Wang Y, et al. Exploring the common pathogenic mechanisms of psoriasis and atopic dermatitis: the interaction between SGK1 and TIGIT signaling pathways. Inflammation. 2025;48(3):1257–69.
8. Matthias J, Maul J, Noster R, et al. Sodium chloride is an ionic checkpoint for human TH2 cells and shapes the atopic skin microenvironment. Sci Transl Med. 2019;11(480):eaau0683.
9. Meng Q, Bai M, Guo M, et al. Inhibition of serum- and glucocorticoid-regulated protein Kinase-1 aggravates Imiquimod-Induced psoriatic dermatitis and enhances proinflammatory cytokine expression through the NF-kB pathway. J Invest Dermatol. 2023;143(6):954–64.
10. Liu H, Wang N, Yang R, et al. E3 ubiquitin ligase NEDD4L negatively regulates skin tumorigenesis by inhibiting IL-6/GP130 signaling pathway. J Invest Dermatol. 2024;144(11):2453–e246411.
11. Jin J, Wang K, Lu C, et al. NEDD4L inhibits the proliferation and migration of keloid fibroblasts by regulating YY1 Ubiquitination-Mediated glycolytic metabolic reprogramming. Exp Dermatol. 2024;33(11):e70008.
12. Liu H, Lin W, Liu Z, et al. E3 ubiquitin ligase NEDD4L negatively regulates keratinocyte hyperplasia by promoting GP130 degradation. EMBO Rep. 2021;22(5):e52063.
13. Chen B, Song Y, Yang X, et al. Bacterial DNA promoting inflammation via the Sgk1/Nedd4L/Syk pathway in mast cells contributes to antihistamine-nonresponsive CSU. J Leukoc Biol. 2023;113(5):461–70.
14. Liu BW, Zhang J, Hong YS, et al. NGF-Induced Nav1.7 upregulation contributes to chronic post-surgical pain by activating SGK1-dependent Nedd4-2 phosphorylation. Mol Neurobiol. 2021;58(3):964–82.
15. Xiao T, Sun M, Zhao C, et al. TRPV1: A promising therapeutic target for skin aging and inflammatory skin diseases. Front Pharmacol. 2023;14:1037925.
16. Marek-Jozefowicz L, Nedoszytko B, Grochocka M, et al. Molecular mechanisms of neurogenic inflammation of the skin. Int J Mol Sci. 2023;24(5):5001.
17. Bao C, Abraham SN. Mast cell-sensory neuron crosstalk in allergic diseases. J Allergy Clin Immunol. 2024;153(4):939–53.
18. Bonchak JG, Swerlick RA. Emerging therapies for atopic dermatitis: TRPV1 antagonists. J Am Acad Dermatol. 2018;788(3 Suppl 1):S63–6.
19. Serhan N, Basso L, Sibilano R, et al. House dust mites activate nociceptor-mast cell clusters to drive type 2 skin inflammation. Nat Immunol. 2019;20(11):1435–43.
20. Zhou GK, Xu WJ, Lu Y, et al. Acid-sensing ion channel 3 is required for agmatine-induced histamine-independent itch in mice. Front Mol Neurosci. 2023;16:1086285.
21. Zhang Y, Zhang M, Tang C, et al. Palmitoylation by ZDHHC4 inhibits TRPV1-mediated nociception. EMBO Rep. 2025;26(1):101–21.
22. He J, Yang J, Chen L, et al. Serum/glucocorticoid-regulated kinase 1-targeted transient receptor potential oxalate subtype 1 regulates bladder smooth muscle cell proliferation due to bladder outlet obstruction in mice via activated T cell nuclear factor transcription factor 2. IUBMB Life. 2022;74(5):463–73.
23. Green DP, Limjunyawong N, Gour N, et al. A Mast-cell-specific receptor mediates neurogenic inflammation and pain. Neuron. 2019;101(3):412–e4203.

24. Liu AW, Zhang YR, Chen CS, et al. Scratching promotes allergic inflammation and host defense via neurogenic mast cell activation. Science. 2025;387(6733):eadn9390.
25. Jia T, Che D, Zheng Y, et al. Mast cells initiate type 2 inflammation through tryptase released by MRGPRX2/MRGPRB2 activation in atopic dermatitis. J Invest Dermatol. 2024;144(1):53–e622.
26. Wang Z, Li Z, Bal G, et al. β-arrestin-1 and β-arrestin-2 restrain MRGPRX2-Triggered degranulation and ERK1/2 activation in human skin mast cells. Front Allergy. 2022;3:930233.
27. Lee S, Park S, Lee H, et al. Nedd4 E3 ligase and beta-arrestins regulate ubiquitination, trafficking, and stability of the mGlu7 receptor. Elife. 2019;8:e44502.
28. Ibáñez I, Díez-Guerra FJ, Giménez C, et al. Activity dependent internalization of the glutamate transporter GLT-1 mediated by β-arrestin 1 and ubiquitination. Neuropharmacology. 2016;107:376–86.
29. Wei C, Lin M, Jinjun B, et al. Involvement of general control nonderepressible kinase 2 in cancer cell apoptosis by posttranslational mechanisms. Mol Biol Cell. 2015;26(2):1044–57.
30. Ning W, Jiang P, Guo Y, et al. GPS-Palm: a deep learning-based graphic presentation system for the prediction of S-palmitoylation sites in proteins. Brief Bioinform. 2021;22(2):1836–47.
31. Chen LY, Yang-Yen HF, Tsai CC, et al. Protein palmitoylation by ZDHHC13 protects skin against microbial-driven dermatitis. J Invest Dermatol. 2017;137(4):894–904.
32. Blaess M, Csuk R, Schätzl T, et al. Elongation of very long-chain fatty acids (ELOVL) in atopic dermatitis and the cutaneous adverse effect AGEP of drugs. Int J Mol Sci. 2024;25(17):9344.
33. Meurer SK, Neß M, Weiskirchen S, et al. Isolation of mature (peritoneum-derived) mast cells and immature (bone marrow-derived) mast cell precursors from mice. PLoS ONE. 2016;11(6):e0158104.
34. Shekarabi M, Robinson JA, Burdo TH. Isolation and culture of dorsal root ganglia (DRG) from rodents. Methods Mol Biol. 2021;2311:177–84.
35. Li F, Adase CA, Zhang LJ. Isolation and culture of primary mouse keratinocytes from neonatal and adult mouse skin. J Vis Exp. 2017;125:56027.
36. Yang J, Xue X, Yang Z, et al. Neural-Inflammation mechanism of spinal palmitic acid promoting atopic dermatitis in mice. J Inflamm Res. 2025;18:7907–19.
37. Hunter DV, Smaila BD, Lopes DM, et al. Advillin is expressed in all adult neural Crest-Derived neurons. eNeuro. 2018;5(5):ENEURO0077–182018.
38. Olejnik A, Gornowicz-Porowska J, Jenerowicz D, et al. Fatty acids profile and the relevance of membranes as the target of nutrition-based strategies in atopic dermatitis: a narrative review. Nutrients. 2023;15(17):3857.
39. van Smeden J, Janssens M, Kaye EC, et al. The importance of free fatty acid chain length for the skin barrier function in atopic eczema patients. Exp Dermatol. 2014;23:45–52.
40. Li T, Wang R, Li R. Fatty acids and mycobiome across skin areas in atopic dermatitis. J Am Acad Dermatol. 2024(Supplement);91(3):AB216. https://doi.org/10.1016/j.jaad.2024.07.858
41. Kim J, Kim BE, Berdyshev E, et al. Staphylococcus aureus causes aberrant epidermal lipid composition and skin barrier dysfunction. Allergy. 2023;78(5):1292–306.
42. Yu J, Song P, Bai Y, et al. CD36-SREBP1 axis mediates TSLP production in obesity-exacerbated atopic dermatitis. J Invest Dermatol. 2023;143(11):2153–e216212.
43. Segawa A, Borges MS, Yokota Y, et al. Suppression of IgE antibody response by the fatty acid-modified antigen. Int Arch Allergy Appl Immunol. 1981;66(2):189–99.
44. Li M, Hener P, Zhang Z, et al. Topical vitamin D3 and low-calcemic analogs induce thymic stromal lymphopoietin in mouse keratinocytes and trigger an atopic dermatitis. Proc Natl Acad Sci U S A. 2006;103(31):11736–41.
45. Xie Y, Takai T, Chen X, et al. Long TSLP transcript expression and release of TSLP induced by TLR ligands and cytokines in human keratinocytes. J Dermatol Sci. 2012;66(3):233–7.
46. Laedermann CJ, Cachemaille M, Kirschmann G, et al. Dysregulation of voltage-gated sodium channels by ubiquitin ligase NEDD4-2 in neuropathic pain. J Clin Invest. 2013;123(7):3002–13.
47. Sun L, Tong CK, Morgenstern TJ, et al. Targeted ubiquitination of sensory neuron calcium channels reduces the development of neuropathic pain. Proc Natl Acad Sci U S A. 2022;119(20):e2118129119.
48. Wang S, Qi S, Kogure Y, et al. The ubiquitin E3 ligase Nedd4-2 relieves mechanical allodynia through the ubiquitination of TRPA1 channel in db/db mice. Eur J Neurosci. 2021;53(6):1691–704.
49. Yu T, Calvo L, Anta B, et al. In vivo regulation of NGF-mediated functions by Nedd4-2 ubiquitination of TrkA. J Neurosci. 2014;34(17):6098–106.
50. Schmid E, Gu S, Yang W, et al. Serum- and glucocorticoid-inducible kinase SGK1 regulates reorganization of actin cytoskeleton in mast cells upon degranulation. Am J Physiol Cell Physiol. 2013;304(1):C49–55.
51. Sobiesiak M, Shumilina E, Lam RS, et al. Impaired mast cell activation in gene-targeted mice lacking the serum- and glucocorticoid-inducible kinase SGK1. J Immunol. 2009;183(7):4395–402.
52. Bury Y, Ruf D, Hansen CM, et al. Molecular evaluation of vitamin D3 receptor agonists designed for topical treatment of skin diseases. J Invest Dermatol. 2001;116(5):785–92.